ENVIRONMENTAL ENGINEERING SCIENCE
Volume 26, Number 6, 2009

DOI: 10.1089/ees.2008.0235

Novel Neural Network-Based Prediction Model for Quantifying Hydroquinone in Compost with Biosensor Measurements

Yi Zhang,[1,*] Wen-Wei Li,[2] Guang-Ming Zeng,[1,*] Lin Tang,[1] Chong-Ling Feng,[1]
Dan-Lian Huang,[1] and Yuan-Ping Li[1]

[1]*College of Environmental Science and Engineering, Hunan University, Changsha, People's Republic of China.*
[2]*School of Chemistry & Material Science, University of Science and Technology of China, Hefei, People's Republic of China.*

Received: July 24, 2008 *Accepted in revised form: January 27, 2009*

Abstract

Hydroquinone generally appears in compost as a direct pollutant or an intermediate product in the aromatic pollutant biodegradation process. The requirement of quantifying its concentration calls for efficient and economical analytical methods. In this study, artificial neural networks (ANNs) were combined with a biosensor to realize nonlinear determination of hydroquinone in a complex composting system. The direct detection range for hydroquinone in compost system using biosensor reached $1.5\times10^{-8} \sim 3.6\times10^{-4}$ M. Meanwhile, the performance of the ANN model was compared with a nonlinear regression model with respect to the simulation accuracy and adaptability to uncertainty, etc. Nonlinear range analysis could extend the usable detection range of biosensor for hydroquinone and could improve the adaptability of the detecting system in real sample determination. Results illustrated that the combined application of biosensor measurement and artificial neural network analysis was a rapid, sensitive, and robust method in a quantitative study of a composting system. This method could be a good analytical tool for further application in real sample determination in other complex environments which refer to human life and health.

Key words: hydroquinone; artificial neural network; biosensor; nonlinear determination; complex compost system

Introduction

PHENOLS, SOME OF WHICH are highly toxic, are important raw materials and byproducts of the large-scale chemical industry (Canofeni *et al.*, 1994). Many of them are resistant to biotic and abiotic degradation in the remediation process. The toxicity of phenols generated from bioremediation, such as composting, can also bring undesirable ecological effects and seriously affect their removal efficiencies (Kulys and Vidziunaite, 2003). Hydroquinone generally appears in the compost as a direct pollutant or an intermediate product in the aromatic pollutant biodegradation process (Canofeni *et al.*, 1994), and has been found to be harmful not only to the environment but also to human health by affecting the central nervous system and causing chromosomal aberration (Topping *et al.*, 2007). With the increasing application of composting technology to the disposal of municipal solid waste (Marques *et al.*, 2008; Quadri *et al.*, 2008), the significance of hydroquinone pollution control is becoming more prominent. Thus, it is a critical issue to quantify the hydroquinone concentration in the composting process of municipal solid waste.

So far, the frequently reported analytical methods in composting systems include spectrophotometry, gas chromatography, and high-performance liquid chromatography (HPLC) (Di Corcia *et al.*, 1996; Faure *et al.*, 1996; Kim and Kim, 2000). However, due to the complexity and uncertainty of the composting system, these methods suffer from drawbacks such as interference by the substrate turbidity and UV-vis-light-absorbing substances, and the cumbrous and time-consuming pretreatment of the sample (Tang *et al.*, 2005). Moreover, the instruments are expensive and heavy. In recent years, biosensor has been widely applied as a detection instrument with superior sensitivity, high stability, reusability, selectivity, portability, and low cost (Forzani *et al.*, 2005; Andreescu and Luck *et al.*, 2008; Drouvalakis *et al.*, 2008; Tang *et al.*, 2008b). Some laccase and tyrosinase biosensors have also been developed to detect phenolic compound and show accurate detecting performance (Kochana *et al.*, 2008; Zhang *et al.*, 2007; Roy *et al.*, 2005).

In our previous study (Zhang *et al.*, 2007), a biosensor based on the immobilization of laccase on the surface of modified

*Corresponding authors: College of Environmental Science and Engineering, Hunan University, Changsha 410082, P.R. China. *Phone:* +86-731-8822754; *Fax:* +86-731-8823701; *E-mail:* ezhangyi123@yahoo.com.cn (YZ), zgming@hnu.cn (GMZ)

magnetic core-shell (Fe_3O_4-SiO_2) nanoparticles was developed for the detection of hydroquinone. Laccase can directly oxidize hydroquinone and utilize dioxygen as an oxidant, reducing it to water. In the reaction, hydroquinone, which was an electron donor for the oxidized form of the enzyme, was mainly converted into quinone and/or free radical product. It was then reduced on the surface of the electrode at potentials below 0 V (vs. SCE), which efficiently shuttled electrons between laccase redox center and the electrode surface in a dynamical equilibrium. The developed biosensor had a linear detection range of $1\times10^{-7} \sim 1.375\times10^{-4}$ M, with a detection limit of 1.5×10^{-8} M (Zhang *et al.*, 2007). Technically, the result is just as well as other hydroquinone sensors. However, when applied to the real-world samples, the biosensor measurement is affected by its linear range. First, the concentration of analyte is uncertain in the real sample, and erroneous results will be given if the concentration of analyte exceeds the linear range (Bessant and Saini, 1999). In addition, the linear range is the normal choice in sensor detection, but generally, the linear range is only a part of the responded signal range; in other words, there is a wide nonlinear range that is not being applied. In fact, there is a nonlinear range of the responded signal range of the biosensor in hydroquinone detection, which is $1.5\times10^{-8} \sim 3.6\times10^{-4}$ M in our previous work (Zhang *et al.*, 2007). If the wide nonlinear range can be fully used, there will be less limitation coming from the linear range, and a more convenient and high-efficient analytical method in practical application will be possible.

Due to their intelligence, artificial neural networks (ANNs) can easily simulate, analyze and solve the nonlinear, overlap and uncertain problems in complex systems. ANNs have been receiving increased attention from many researchers. Some researchers have successfully coupled ANN with sensor as a chemometric tool for analyzing a complex system, the ANN showed a strong, nonlinear mapping and self-learning ability to cope with complex data. ANN introduced into biosensor analysis hither to was mainly used to analyze the target analyte of biosensor array or the multiple analytes of a single biosensor with high accuracy and correlativity in comparison with linear regression models (Hasani *et al.*, 2007; Gutés *et al.*, 2005a, 2005b; Gutiérrez *et al.*, 2007; Ni *et al.*, 2005; Tang *et al.*, 2006). Tang *et al.* (2008a) applied a laccase sensor and artificial neural networks in catechol determination, and the architecture of ANN was built with 12 input neurons directly taken from data points of each amperometric curve before the detection current reached steady state. As an extension of our previous efforts, a feed-forward backpropagation–ANN model was developed based on the relationship between hydroquinone concentrations and response currents of biosensor. Different from Tang *et al.*'s work (2008a), we adopted the current stabilizing time, steady-state current and three characteristic values of response currents of biosensor to build the ANN, which resulted in a completely different network construction. A different nonlinear regression model was also developed in our study for comparison with the performance of the ANN model. The nonlinear range analysis was completed to extend the direct detection range of biosensor for hydroquinone in a complex composting system. Coupled with the inherent high sensitivity, rapidity, robustness and portability of an electrochemical sensor technique, the presented method enables the development of a fast and inexpensive on-line monitoring system in industrial waste composting and bioremediation.

Materials and Methods

Reagents and materials

Laccase (EC 1.10.3.2, 23.3 U/mg) was purchased from Fluka. Tetraethoxysilane (TEOS), 3-aminopropyltriethoxysilane (APTES), polyethylene glycol (PEG), and all other chemicals were of analytical grade and used as received. The preparation of carbon paste electrode, synthesis of Fe_3O_4 magnetic nanoparticles and the immobilization of laccase on the surface of nanoparticles were implemented in the same way as introduced by Zhang *et al.* (2007).

Hydroquinone measurements in compost extracts

The HPLC and amperometric measurements of hydroquinone concentration were applied using compost sample extracts. The composting process was carried out as described in our previous work (Zeng *et al.*, 2004). Ten grams of compost sample were extracted with 200 mL water by agitating at 200 rpm for 2 h. The supernatant was centrifuged to obtain the compost extract. The dosage of hydroquinone into each compost extract was controlled. Hydroquinone concentration was then measured by HPLC method under the following conditions: the eluent consisted of an isocratic mixture of water, acetonitrile, and acetic acid (88:10:2) at flow rate of $0.7\,mL\cdot min^{-1}$, and the concentration of hydroquinone was detected by ultraviolet spectrophotometer at 280 nm (Chapuis-Lardy *et al.*, 2002). The electrochemical measurements of hydroquinone concentration were performed on CHI660B electrochemistry system (Chenhua Instrument, Shanghai, China). The three-electrode system used in this work consisted of a carbon paste electrode (diameter of 8 mm) as working electrode of interest, a saturated calomel electrode (SCE) as reference electrode and a Pt foil auxiliary electrode. As the optimization results of the amperometric monitoring system, the electrolyte was 30 mL $67\,mmol\cdot L^{-1}$ phosphate buffer (pH 5.5) containing hydroquinone, and the oxidation peak potential was −0.232 V (vs. SCE) for the highest sensitivity of the enzyme sensor.

Application of ANN models

As shown in Fig. 1, ANN models were applied to analyze the measured hydroquinone concentrations in compost samples and the corresponding amperometric response of biosensor. The measurement data were divided into two parts: one for prediction, and the other for model validation. The data from 25 compost extract samples were used to train the ANN network, as shown in Fig. 2. Other 14 extract sample measurements were applied to estimate the modeling performance. The data from other 12 extract samples were used to validate the ANN model application.

Matlab 7.0 (Mathworks, Natick, MA), its Neural Network Toolbox in particular, was employed to develop the backpropagation-ANN (BP-ANN) models. Of the various existing ANN architectures, the multilayer feedforward backpropagation network defines one of the most widely and successfully used algorithms (Schäfer *et al.*, 2007). It consists of one input layer, one output layer, and one or more hidden layers (Looner, 1997). As a good pattern classifier, signal filter and data compressor, this type of network was widely adopted (Torrecilla *et al.*, 2007). Specifically, the backpropagation network is applied to model systems based

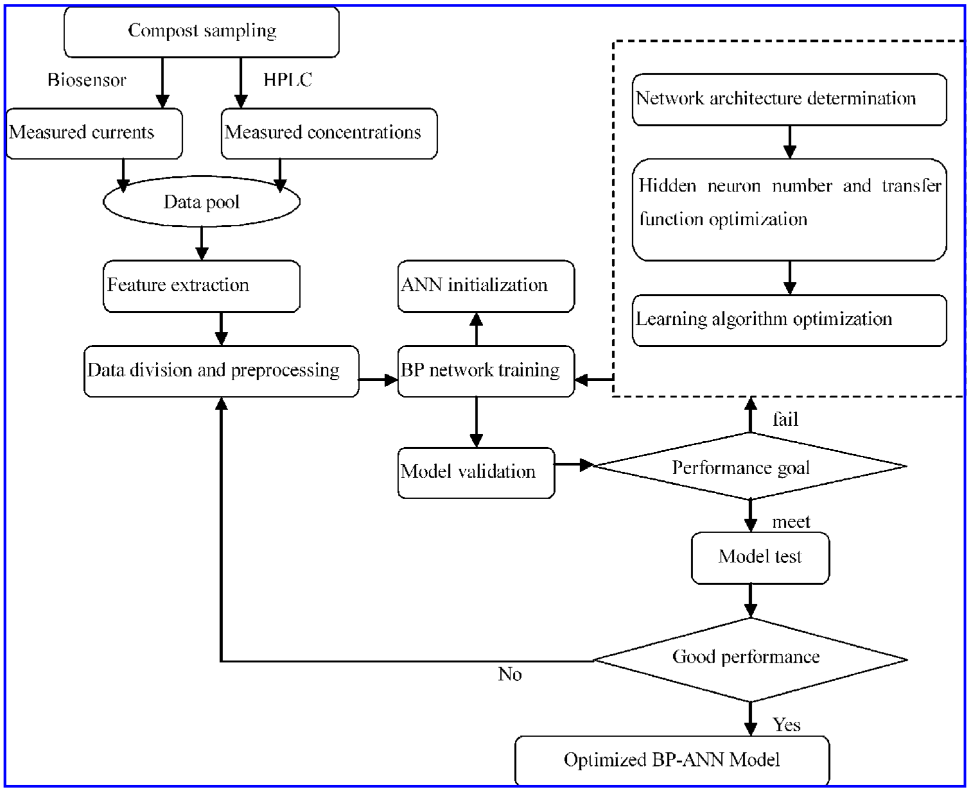

FIG. 1. Schematic diagram of the system based on the artificial neural network (ANN) model and biosensor. HPLC, high-performance liquid chromatography; BP, backpropagation.

on nonlinear dynamics, while the knowledge of the to-be-modeled system is not necessarily required. Therefore, ANN has enormous applicability (Torrecilla *et al.*, 2007).

Results and Discussion

Construction of neural network based prediction model

In this paper, ANN was combined with the biosensor to detect hydroquinone in compost. The current stabilizing time,

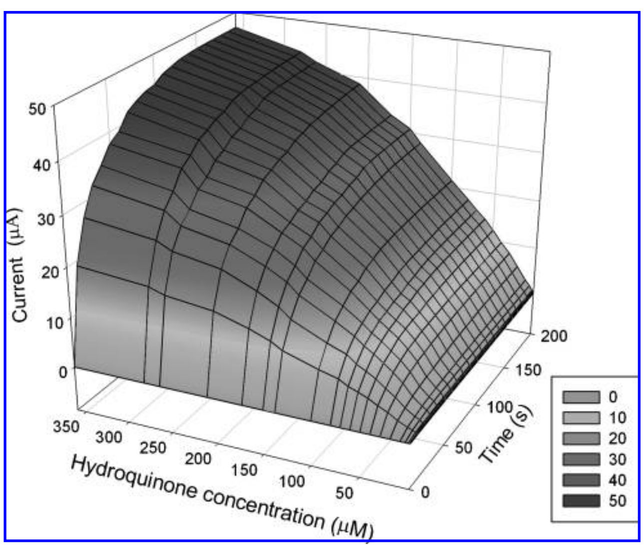

FIG. 2. Related information of 25 compost extract samples for the training network. Hydroquinone concentration for training set is between 0.15 μM and 360 μM.

steady-state current and three characteristic values of response current after feature extraction were adopted as the input vectors. These five vectors contained an intact structure of characteristic curve and the correlation factors to function with the ANN reasonably.

First, the response current was analyzed to find out the characteristic values A_1, A_2, A_3, and obtain an equation that could describe the features of the response current.

$$y = A_1x^2 + A_2x + A_3 \quad (1)$$

where y is the response current and x is the response time.

Next, the other two factors (current stabilizing time and steady-state current) were introduced into the ANN running as the input vectors which kept the input information intact. Generally, the current stabilizing time was proportional to the analyte concentration in electrochemical sensor determination. The change of the stabilizing time with different concentrations of different analytes exhibited some available information, that is, a correlation exists between concentration and corresponding stabilizing time. Moreover, the steady-state current could reflect the response result directly. The five factors could represent all characters and relations between the response current and the analyte concentration, which formed an intact and scientific structure to perform a piece of accurate information of the response current.

In the experiment, under the optimum condition, different curves of current vs. time were obtained corresponding to the hydroquinone concentrations. The concentration of hydroquinone in the compost extracts varied from 1.5×10^{-8} to 3.6×10^{-4} M. The concentration of hydroquinone is the target for ANN modeling with a single hidden layer. It was reported that an ANN with the single hidden layer mapping structure,

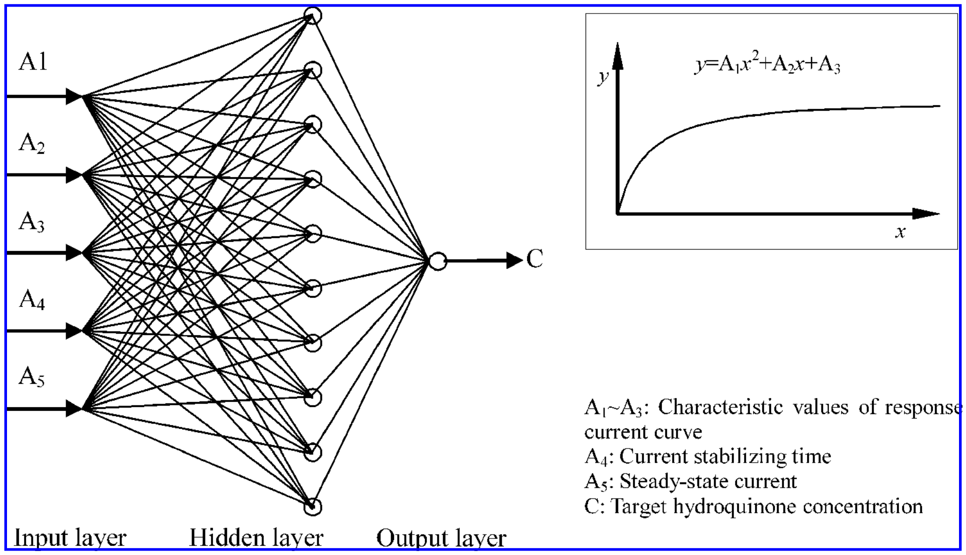

FIG. 3. Example of the ANN architecture used to interpret amperometric responses.

one input layer and one output layer, could resolve the nonlinear problem that appeared in electrochemical signal analysis process in the relative literature (Gutés *et al.*, 2005c). Therefore, networks with more than one hidden layer were not considered in this paper. The architecture of BP-ANN is shown in Fig. 3.

Network performance

Feed-forward backpropagation with random initial weights and biases to avoid selecting fixed conditions was used to train the networks, which might favor one particular network design. An exhaustive study of the network model structure was done to optimize the determination of hydroquinone concentration. The network performance was quantified by calculating the root mean square of error (RMSE) between the expected and predicted hydroquinone concentration for the parameter set. The calculating formula of RMSE (μM) is

$$\mathrm{RMSE} = \sqrt{\sum (a_i - \hat{a}_i)^2 / n} \tag{2}$$

where a_i and $\hat{a}_i$ are, respectively, the predicted and the expected concentrations by the ANN, and n is the number of the test samples.

Variability will occur owing to random initial values of connection weights during network training with the exactly same programme (Bachmann *et al.*, 2000). Therefore, each ANN programme was run more than five times, and the RMSEs for the external test sets were averaged.

Generally, four fundamental types of transfer functions were usually utilized for hidden and output layers in ANNs modeling, namely, hyperbolic tangent sigmoid transfer function (Tansig); logistic sigmoid transfer function (Logsig); linear transfer function (Purelin) and symmetric saturating linear transfer function (Satlins). Sigmoid functions, due to their powerful nonlinear approach capability, are often used in hidden layers. As to the output of transfer function, the range of Tansig is $(-1, 1)$, Logsig is $(0, 1)$, Purelin is $(-\infty, \infty)$, and the output of Satlins lies in the range of $[-1, 1]$. In the modeling, the input and output data sets were normalized and the range of the output in the sample set is in $(0, 1)$.

The ability of nonlinear approach of BP-network commonly was realized by sigmoid transfer function. A BP-network was built with Levenberg–Marquardt backpropagation (trainlm) as optimization algorithm and five data vectors as the inputs. According to Kolmogorov's theory (Nielson, 1989), hidden neuron number usually takes a formula with

$$n_2 = \sqrt{(n_1 + m + 1) + a} \tag{3}$$

where n_2, n_1, and m represent the numbers of hidden neuron, input neuron, and output neuron, respectively; a = 1. . .10. To determine the optimal hidden neuron number, the performances of the network under different transfer function combinations and hidden neuron numbers on the network performance were studied synchronously. The RMSEs were calculated with different transfer function combinations in the hidden and output layers and 10 neuron gradients ($4 \sim 13$) in the hidden layer to optimize the transfer function and neuron number. It was found that the training process with Purelin in the output layer could not meet the performance goal when the minimum gradient was reached, resulting in large RMSEs. According to Fig. 4, the comparison of the transfer function combinations of Tangsig–Satlin, Logsig–Satlin, Tangsig–Logsig, and Logsig–Logsig showed that the network with Logsig–Logsig gave slightly lower RMSE values, but the difference was not significant. However, the lowest RMSE value was obtained with 10 hidden neurons and Logsig-Logsig as transfer function combination, shown in Fig. 4.

Next, the effects of the different optimization algorithms with five input neuron numbers on the model performance were evaluated and optimized in parallel. As shown in Fig. 5, BFGS quasi-Newton method (trainbfg), Bayesian regularization backpropagation (trainbr), Levenberg-Marquardt backpropagation (trainlm), gradient descent with momentum backpropagation (traingdm), gradient descent backpropagation (traingd), gradient descent with momentum and adaptive learning rate backpropagation (traingdx) and conjugate gradient backpropagation with Powell-Beale restarts (traincgb) were respectively applied to the ANN modeling. The RMSEs represented the performances of the models with different input neuron numbers and algorithms under optimal transfer

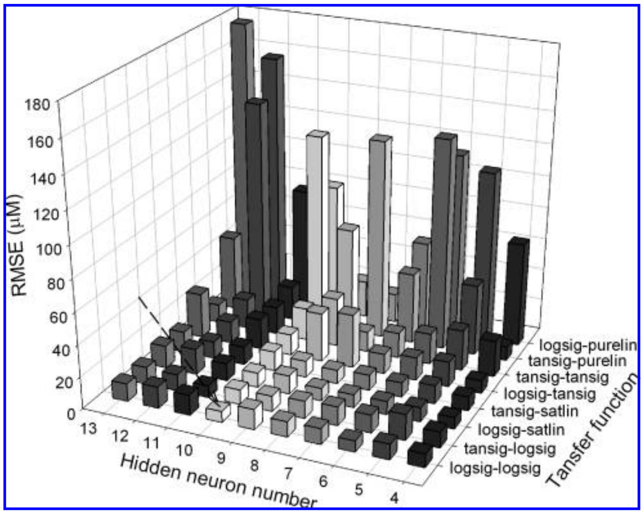

FIG. 4. Root mean squares of error (RMSEs) in hydroquinone concentration prediction for different function combinations and neuron numbers in the hidden layer with input neuron number of 5 and Levenberg–Marquardt backpropagation (trainlm) as optimization algorithm.

function combination of Logsig-Logsig and hidden neuron number of 10. The ANN models with trainbfg, traingdm, traingd, and traincgb as algorithms, respectively, could not meet the performance goal when the minimum gradient was reached in the training process. Therefore, those algorithms were not taken into account. Although trainbr and traingdx could get lower RMSE values sometimes, the results were not steady with the increasing training time. Contrarily, trainlm not only showed the lowest RMSE value, but also exhibited stability in its results. So trainlm was selected as the optimal algorithm to obtain the lowest RMSE value. In this study, the inputs were the five factors referred hereinbefore for each independent sample. For the network prediction accuracy, we can increase the number of training data sets or number of data points in each set. However, there are drawbacks of adopting too many samples. It will result in a poor generalization by the network and increase training time. Likewise, there are also limitations associated with selecting too few samples, which will lead to the inability of the network to train successfully. Therefore, taking the complexity of the model and economical training time into account, adequate data were selected for adequate accuracy of simulation in our study. The fixed number of five inputs not only contained intact information, but also saved the ANN running time to get an efficient operation.

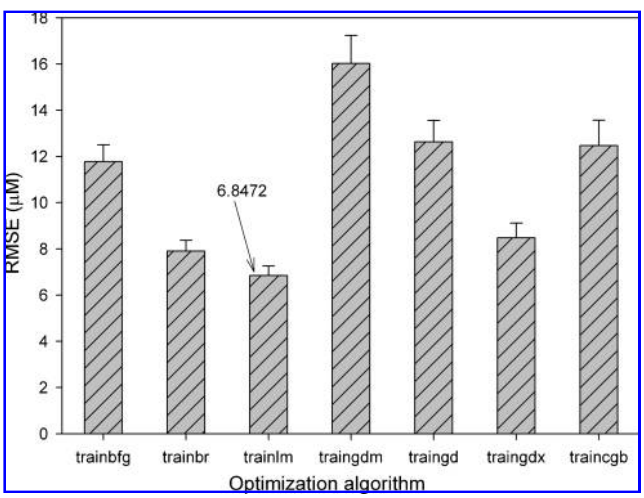

FIG. 5. RMSEs in hydroquinone concentration prediction for different optimization algorithms with the optimal transfer function combination of Logsig-Logsig and hidden neuron number of 10.

In order to obtain accurate hydroquinone concentrations from ANN models, triplicate calculation results of the optimized network was averaged, the RMSEs of 6.8472 for hydroquinone concentration was achieved. The final optimization results of ANN model are shown in Table 1.

Comparison of prediction results between nonlinear regression model and ANN model in composting system

The performance of the ANN model was compared with the regression model in respect to correlation coefficient, adaptability to uncertainty, etc. The equation of nonlinear regression model is:

$$y = 0.8333x^3 - 1.8577x^2 + 2.0437x - 0.0405 \tag{4}$$

where y is hydroquinone concentration (μM), x is the response current value (μA), and $R^2 = 0.9778$. The nonlinear regression model and ANN model here were applied to predict hydroquinone concentration in 12 compost extract samples separately.

Figure 6 showed the correlation between the experimental and predicted values of nonlinear regression model and ANN model, and there was a nonlinearity in the hydroquinone concentration range of $1.5\times10^{-8} \sim 4.5\times10^{-4}$ M. The fitting degree of ANN with high correlation coefficients ($R^2 = 0.9957$) excelled the nonlinear regression model's ($R^2 = 0.9778$). It was indicated that the predicted values by ANN fit better to the experimental value than those of the nonlinear regression model. It is not difficult to identify the factors which can account for this result. First, ANN, owing to its powerful prediction ability, is able to enlarge determining limit, from $1\times10^{-7} \sim 1.375\times10^{-4}$ M to $1.5\times10^{-8} \sim 3.6\times10^{-4}$ M, by making use of data in a wider scope, and meanwhile improve the

Table 1. Optimal Results of Artificial Neural Network Architecture and Training Parameters

Architecture/parameter	*Value*
Input neuron number	5
Hidden neuron number	10
Transfer function in the hidden layer	Logsig
Output neuron number	1
Transfer function in the output layer	Logsig
Optimization algorithm	Levenberg-Marquardt backpropagation (trainlm)
RMSE for hydroquinone concentration (μM)	6.8472

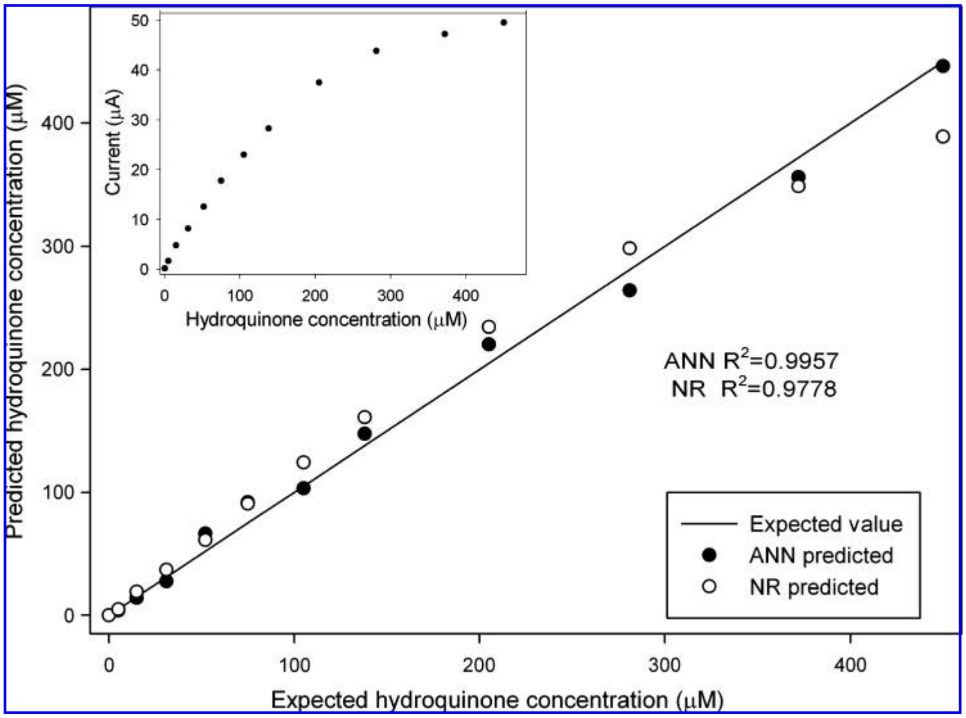

FIG. 6. Expected hydroquinone concentration measured by high-performance liquid chromatography against those predicted by the nonlinear regression (NR) model for compost extract samples. Inset: the plot of current versus hydroquinone between 0.18 μM and 450 μM.

determination accuracy and analysis efficiency. Thus, ANN combining with biosensor technology turned out to be an efficient analytical tool to avoid this problem and achieve more convenient and applicable detection. Second, the ascendancy of ANN is of particular prominence in the relatively high concentration range. The linear range of the linear model for hydroquinone determination in our previous work was only $1\times10^{-7} \sim 1.375\times10^{-4}$ M (linear detection range), while the detection range which the ANN model could direct analyze amounted to $1.5\times10^{-8} \sim 3.6\times10^{-4}$ M (nonlinear detection range), which is wider than the other hydroquinone sensors (Vianello *et al.*, 2004; Jarosz-Wilkołazka *et al.*, 2005; de Oliveira *et al.*, 2007). A nonlinear detection range is superior to a linear one, as it is difficult even impossible to judge whether a concentration is in the linear range in practice. Therefore, the risk of inaccurate calculation can be reduced by application of the nonlinear detection range. With that, ANN offers better performances than the other hydroquinone sensors in detecting the real samples. Last but not least, due to the black-box approach that depends only on the observed values, ANN can easily describe the complicated phenomenon in the complex compost system, and therefore, simplify the detection.

Therefore, as the results indicated, ANNs were superior to the nonlinear regression model and traditional linear regression for the hydroquinone concentration determination in compost system. Combined with the ANN model, the direct detection range for hydroquinone in a compost system of the biosensor was widened and nonlinear determination was achieved. This combination would enhance the performance of the detection system in further application in real compost extract sample determination.

The practicability of the biosensor to determine hydroquinone in the complex compost system has been verified in our previous work (Zhang *et al.*, 2007). We introduced the ANN into the detection system to advance its performance and then built an on-line system of detection and prediction as a chemometric tool to determine the hydroquinone concentration in compost system more effectively. Based on ANNs' strong learning and prediction capability, it can be applied to treat the nonlinear, dynamic, and uncertain properties of the complex composting system, which cannot be treated by regression models. The combination of the two techniques advanced the detection performance and was expected to make it more effective in practical application.

Conclusions

Hydroquinone harms human health and environment, and it is practically significant to detect hydroquinone in environmental sample. An on-line system of detection and prediction by artificial neural networks as a chemometric tool was developed to determine hydroquinone in compost system more effectively. Due to the nonlinear determination, the direct detection range for hydroquinone in the compost system of the biosensor was extended to $1.5\times10^{-8} \sim 3.6\times10^{-4}$ M, which was superior to other hydroquinone sensors. This would enhance the performance of the detection system in further application in real compost-extracted sample determination. The performance superiority of the ANN model was displayed by comparing the nonlinear regression model with respect to simulation accuracy and adaptability to uncertainty, etc. The results showed that this biosensor combined with the ANN model could be a good analytical tool for further application in real sample determination in other complex environments.

Acknowledgments

The study was financially supported by the National Natural Science Foundation of China (No. 50608029), the National

863 High Technologies Research Foundation of China (No. 2004AA649370), the National Basic Research Program (973 Program) (No. 2005CB724203), Program for Changjiang Scholars and Innovative Research Team in University (PCSIRT), and the Natural Foundation for Distinguished Young Scholars (No. 50425927, No. 50225926).

Author Disclosure Statement

The authors declare that no competing financial interests exist.

References

Andreescu, S., and Luck, L.A. (2008). Studies of the binding and signaling of surface-immobilized periplasmic glucose receptors on gold nanoparticles: A glucose biosensor application. *Anal. Biochem.* 375, 282.

Bachmann, T.T., Leca, B., Vilatte, F., Marty, J.L., Fournier, D., and Schmid, R.D. (2000). Improved multianalyte detection of organophosphates and carbamates with disposable multielectrode biosensors using recombinant mutants of *Drosophila* acetylcholinesterase and artificial neural networks. *Biosens. Bioelectron*. 15, 193.

Bessant, C., and Saini, S. (1999). Simultaneous determination of ethanol, fructose, and glucose at an unmodified platinum electrode using artificial neural networks. *Anal. Chem.* 71, 2806.

Canofeni, S., Sario, S.D., Mela, J., and Pilloton, R. (1994). Comparison of immobilization procedures for development of an electrochemical ppobased biosensor for online monitoring of a depuration process. *Anal. Lett.* 27, 1659.

Chapuis-Lardy, L., Contour-Ansel, D., and Bernhard-Reversat, F. (2002). High-performance liquid chromatography of water-soluble phenolics in leaf litter of three *Eucalyptus* hybrids (Congo). *Plant Sci.* 163, 217.

De Oliveira, I.R.W.Z., and De Barros Osório, R.E.M., Neves, A., and Vieira, I.C. (2007). Biomimetic sensor based on a novel copper complex for the determination of hydroquinone in cosmetics. *Sensor. Actuat. B* 122, 89.

Di Corcia, A. Bellioni, A., Madbouly, M.D., and Marchese, S. (1996). Trace determination of phenols in natural waters extraction by a new graphitized carbon black cartridge followed by liquid chromatography and re-analysis after phenol derivatization. *J. Chromatogr. A* 733, 383.

Drouvalakis, K.A., Bangsaruntip, S. Hueber, W., Kozar, L.G., Utz, P.J., and Dai, H. (2008). Peptide-coated nanotube-based biosensor for the detection of disease-specific autoantibodies in human serum. *Biosens. Bioelectron.* 23, 1413.

Faure, D., Bouillant, M.L., Jacoud, C., and Bally, R. (1996). Phenolic derivatives related to lignin metabolism as substrates for *Azospirillum* laccase activity. *Phytochemistry* 42, 357.

Forzani, E.S., Zhang, H., Chen, W., and Tao, N. (2005). Detection of heavy metal ions in drinking water using a high-resolution differential surface plasmon resonance sensor. *Environ. Sci. Technol.* 39, 1257.

Gutés, A., Céspedes, F., Alegret, S., and Del Valle, M. (2005a). Determination of phenolic compounds by a polyphenol oxidase amperometric biosensor and artificial neural network analysis. *Biosens. Bioelectron.* 20, 1668.

Gutés, A., Céspedes, F., Alegret, S., and Del Valle, M. (2005b). Sequential injection system with higher dimensional electrochemical sensor signals: Part 1. Voltammetric e-tongue for the determination of oxidizable compounds. *Talant* 66, 1187.

Gutés, A., Céspedes, F., Alegret, S., and Del Valle, M. (2005c). Simultaneous determination of phenolic compounds by means of an automated voltammetric "electronic tongue." *Anal. Bioanal. Chem.* 382, 471.

Gutiérrez, M., Alegret, S., and Del Valle, M. (2007). Potentiometric bioelectronic tongue for the analysis of urea and alkaline ions in clinical samples. *Biosens. Bioelectron.* 22, 2171.

Hasani, M., Yaghoubi, L., and Abdollahi, H. (2007). A kinetic spectrophotometric method for simultaneous determination of glycine and lysine by artificial neural networks. *Anal. Biochem.* 365, 74.

Jarosz-Wilkołazka, A., Ruzgas, T., and Gorton, L. (2005). Amperometric detection of mono- and diphenols at Cerrena unicolor laccase-modified graphite electrode: correlation between sensitivity and substrate structure. *Talanta* 66, 1219.

Kim, K.R., and Kim, H. (2000). Gas chromatographic profiling and screening for phenols as isobutoxycarbonyl derivatives in aqueous samples. *J. Chromatogr. A* 866, 87.

Kochana, J., Nowak, P., Jarosz-Wilkołazka, A., and Bieroń, M. (2008). Tyrosinase/laccase bienzyme biosensor for amperometric determination of phenolic compounds. *Microchem. J.* 89, 171.

Kulys, J., and Vidziunaite, R. (2003). Amperometric biosensors based on recombinant laccases for phenols determination. *Biosens. Bioelectron.* 18, 319.

Looner, C.G. (1997). *Pattern Recognition Using Neural Networks, Theory and Algorithms for Engineers and Scientists.* New York: Oxford University Press.

Marques, A.P.G.C., Oliveira, R.S., Rangel, A.O.S.S., and Castro, P.M.L. (2008). Application of manure and compost to contaminated soils and its effect on zinc accumulation by *Solanum nigrum* inoculated with arbuscular mycorrhizal fungi. *Environ. Pollut.* 151, 608.

Ni, Y. Qiu, P., and Kokot, S. (2005). Simultaneous voltammetric determination of four carbamate pesticides with the use of chemometrics. *Anal. Chim. Acta* 537, 321.

Nielson, R.H. (1989). Theory of the back propagation neural network. *IEEE Int. Joint Conf. Neural Networks* 1, 593.

Quadri, G., Chen, X., Jawitz, J.W., Tambone, F., Genevini, P., Faoro, F., and Adani, F. (2008). Biobased surfactant-like molecules from organic wastes: The effect of waste composition and composting process on surfactant properties and on the ability to solubilize tetrachloroethene (PCE). *Environ. Sci. Technol.* 42, 2618.

Roy, J.J., Abraham, T.E., Abhijith, K.S., Kumar, P.V. S., and Thakur, M.S. (2005). Biosensor for the determination of phenols based on cross-linked enzyme crystals (CLEC) of laccase. *Biosens. Bioelectron.* 21, 206.

Schäfer, D., Maciejwska, M., and Schuhmann, W. (2007). SECM visualization of spatial variability of enzyme–polymer spots: 1. Discretisation and interference elimination using artificial neural networks. *Biosens. Bioelectron.* 22, 1887.

Tang, L., Zeng, G.M., Liu, J.X., Xu, X.M., Zhang, Y., Shen, G.L., Li, Y.P., and Liu, C. (2008a). Catechol determination in compost bioremediation using a laccase sensor and artificial neural networks. *Anal. Bioanal. Chem.* 391, 679.

Tang, L., Zeng, G.M., Shen, G.L., Li, Y.P., Zhang, Y., and Huang, D.L. (2008b). Rapid detection of picloram in agricultural field samples using a disposable immunomembrane-based electrochemical sensor. *Environ. Sci. Technol.* 42, 1207.

Tang, L., Zeng, G.M., Shen, G.L., Zhang, Y., Huang, G.H., and Li, J.B. (2006). Simultaneous amperometric determination of lignin peroxidase and manganese peroxidase activities in compost bioremediation using artificial neural networks. *Anal. Chim. Acta* 579, 109.

Tang, L., Zeng, G.M., Wang, H., Shen, G.L., and Huang, D.L. (2005). Amperometric detection of lignin-degrading peroxidase activities from *Phanerochaete chrysosporium. Enzyme. Microb. Tech*. 36, 960.

Topping, D.C., Bernard, L.G., O'Donoghue, J.L., and Caroline English, J. (2007). Hydroquinone: Acute and subchronic toxicity studies with emphasis on neurobehavioral and nephrotoxic effects. *Food Chem. Toxicol.* 45, 70.

Torrecilla, J.S., Mena, M.L., Yáñez-Sedeño, P., and García, J. (2007). Application of artificial neural network to the determination of phenolic compounds in olive oil mill wastewater. *J. Food Eng*. 81, 544.

Vianello, F., Cambria, A., Ragusa, S., Cambria, M.T., Zennaro, L., and Rigo, A. (2004). A high sensitivity amperometric biosensor using a monomolecular layer of laccase as biorecognition element. *Biosens. Bioelectron.* 20, 315.

Zeng, G.M., Tang, L., Shen, G.L., Huang, G.H., and Niu, C.G. (2004). Determination of trace chromium(VI) by an inhibition-based enzyme biosensor incorporating an electropolymerized aniline membrane and ferrocene as electron transfer mediator. *Int. J. Environ. An. Ch.* 84, 761.

Zhang, Y., Zeng, G.M., Tang, L., Huang, D.L., Jiang, X.Y., and Chen, Y.N. (2007). A hydroquinone biosensor using modified core–shell magnetic nanoparticles supported on carbon paste electrode. *Biosens. Bioelectron*. 22, 2121.